electrons would be (8)(0.025)(24) = 4.8 e.v. If there is a gain of say 5.6 e.v. in bonding, there is a profit of 0.8 e.v. All the figures are of course only illustrative, but they indicate that an appreciable net gain in bond energy by $p\pi$-$d\pi$ hybridization is not unreasonable.

It should be especially noted that the *gain* in bond energy by hybridization goes linearly with β (*cf.* eq. 10), while the *cost* goes as β^2. Hence if β^2 is sufficiently small the gain will certainly exceed the cost.

Single bonds in Br_2 and I_2 should be strengthened in a way similar to that for Cl_2 by d hybridization, as should also S–S, P–P and other second-row and higher-row single bonds.

Acknowledgment.—The writer is indebted to Dr. L. E. Orgel for reading the manuscript and for pointing out the desirability of a discussion here of the importance and justification of the use of "unnatural" atomic orbitals with increased Z values in hybridization.

CHICAGO, ILLINOIS

[CONTRIBUTION FROM THE LABORATORY OF MOLECULAR STRUCTURE AND SPECTRA, DEPARTMENT OF PHYSICS, THE UNIVERSITY OF CHICAGO]

Bond Angles in Water-Type and Ammonia-Type Molecules and Their Derivatives[1]

BY R. S. MULLIKEN

RECEIVED AUGUST 12, 1954

The factors which may determine the smaller bond angles in the hydrides of the higher-row fifth-column and sixth-column atoms as compared with NH_3 and H_2O, and the much larger energies required to flatten PH_3 and AsH_3 to planar form than for NH_3, are discussed using LCAO molecular orbital and valence bond theory. It is shown that the observed differences can reasonably be understood as a result of d hybridization in the e-type or b_2-type bonding molecular orbitals, together perhaps with smaller nonbonded repulsions between H atoms, in the higher-row hydrides. Significant factors affecting the bond angles in the halides of fifth-column and sixth-column atoms are also surveyed.

Introduction

According to quantum-mechanical valence-bond theory in its simplest form, the bonds in molecules such as H_2O, H_2S, . . ., and their derivatives and NH_3, PH_3, . . ., and their derivatives should make 90° angles with one another for pure p-electron valence. The actual observed angles are usually considerably greater (see Table I for some examples).[2] This fact can be understood qualitatively in terms of partial s, p hybridization, non-bonded repulsions between H (or other substituted) atoms, and other factors.[3,4] However, no adequate explanation seems to have been offered as to why H_2S, H_2Se, . . ., and PH_3, AsH_3, . . ., have angles close to 90° when their first-row analogs H_2O, NH_3 do not,[5,6] nor why the energy required to make NH_3 planar (0.26 e.v.) is so much smaller than for PH_3 (1.3 e.v.) or AsH_3 (1.5 e.v.).[2b] What seems to be a reasonable explanation is presented below. Some discussion of the lack of corresponding differences for substituted compounds (*e.g.*, PF_3 as against NH_3) is also given.

TABLE I

BOND ANGLES IN RH_2, RX_2, RH_3 AND RX_3 MOLECULES

H_2O: 105° 3′	F_2O: 101°	Cl_2O: 110.8°		
H_2S: 92° 16′		Cl_2S: 102°		
H_2Se: ~90°			Br_2Te: 98°	
NH_3: 106° 46′	NF_3: 102° 9′			
PH_3: 93° 18′	PF_3: 102°	PCl_3: 100° 7′	PBr_3: 101°	PI_3: 100°
AsH_3: 91° 30′	AsF_3: 102°	$AsCl_3$: 98° 25′	$AsBr_3$: 101°	AsI_3: 100.5°
SbH_3: 91° 30′		$SbCl_3$: 99.5°	$SbBr_3$: 97°	SbI_3: 98.5°

Fifth-Column Hydrides

The non-localized MO (molecular orbital) structures of hydrides of the type AH_n have been described qualitatively in earlier papers.[7] For NH_3 the structure is

$$\text{Pyramidal } NH_3\text{: } (1a_1)^2(2a_1)^2(1e)^4(3a_1)^2 \qquad (1)$$
$$\qquad\qquad\qquad\qquad\qquad\qquad\qquad\qquad\qquad\qquad B \quad B$$

(1) This work was assisted in part by the Office of Scientific Research, Air Research and Development Command, under Project R-351-40-4 of Contract AF 18(600)-471 with The University of Chicago.

(2) For references on bond angles, *cf.* (a) A. D. Walsh, *J. Chem. Soc.*, 2266 (1953); G. Herzberg, "Infrared and Raman Spectra," Van Nostrand Co., New York, N. Y., 1945; (b) R. E. Weston, THIS JOURNAL, **76**, 2645 (1954); (c) P. Kisliuk, *J. Chem. Phys.*, **22**, 86 (1954).

(3) See D. F. Heath and J. W. Linnett, *Trans. Faraday Soc.*, **44**, 556 (1947), on H_2O; D. F. Heath, J. W. Linnett and Wheatley, *ibid.*, **46**, 137 (1950), on H_2O, H_2S, H_2Se, NH_3, AsH_3, CH_4, etc.; T. Simanouti, *J. Chem. Phys.*, **17**, 245, 734 (1949); D. F. Heath and J. W. Linnett, *ibid.*, **18**, 147 (1950); J. Duchesne and I. Ottelet, *ibid.*, **17**, 1354 (1949); *J. Phys. Rad.*, **11**, 119 (1950). Also ref. 2c.

(4) A. D. Walsh, *J. Chem. Soc.*, 2260 (1953). However, Walsh's assumption that A atom s-pz hybridization is absent in the MOs of AH_2 and AB_2 molecules for a 90° bond angle cannot be accepted.

(5) However, C. A. Burns, Jr., and W. Gordy [*Phys. Rev.*, **92**, 274 (1953)] in order to account for observed asymmetry in nuclear quadrupole coupling in H_2S, have postulated considerable amounts of d as well as s hybridization, and state that qualitative estimates indicate that such hybridization is in harmony with the observed bond angle.

(6) Linnett and Poš (*Trans. Faraday Soc.*, **47**, 1033 (1951)) have emphasized that the bond angles in NH_3 and H_2O approximate to those for tetrahedral hybrid valence, and have made calculations which favor this view (but see T.-Y. Wu, *J. Chem. Phys.*, **22**, 1125 (1954)). Refinement of the same calculations and their extension to PH_3 by Mellish and Linnett (*Trans. Faraday Soc.*, **50**, 657 (1954)), predict close approximation to tetrahedral angles for PH_3 as well as NH_3, in disagreement with what is observed.

(7) R. S. Mulliken, *J. Chem. Phys.*, **1**, 492 (1933); **3**, 506 (1935).

The MOs in (1) are listed in order of increasing energy, with the principal bonding MOs marked B; the rest are non-bonding or nearly so. All the MOs are classified according to their group-theoretical species for the observed pyramidal symmetry (C_{3v}). It will be helpful also to consider the electronic structure which NH_3 would have if it were flattened to a planar form (symmetry D_{3h}).

$$\text{Planar } NH_3\text{: } \underset{B}{(1a_1')^2}\underset{B}{(2a_1')^2}(1e')^4(1a_2'')^2 \qquad (2)$$

For convenient reference, the group-theory tables defining the MO species for symmetries D_{3h} and C_{3v} are given in Table II, and their correlation when the symmetry is reduced from D_{3h} to C_{3v} is shown.

TABLE II

GROUP-THEORETICAL SPECIES FOR SYMMETRIES D_{3h} AND C_{3v}

D_{3h}	I	$2C_3$	$3C_2$	σ_h	$3\sigma_v$	C_{3v}	I	C_3	$3\sigma_v$
a_1'	1	1	1	1	1	a_1	1	1	1
a_2''	1	1	−1	−1	1				
a_2'	1	1	−1	1	−1	a_2	1	1	−1
a_1''	1	1	1	−1	−1				
e'	2	−1	0	2	0	e	2	−1	0
e''	2	−1	0	−2	0				

The forms of the MOs in (1) and (2), in LCAO approximation, are

$$\text{pyramidal } NH_2\ (C_{3v}) \begin{cases} ma_1 = \alpha_{mk}1s_N + \alpha_{ms}2s_N + \alpha_{mz}2pz_N + \alpha_{mh}a_1(H_3) \\ 1e = \beta_p 2p\pi_N + \beta_h e(H_3) \end{cases} \qquad (3)$$

$$\text{planar } NH_3(D_{3h}) \begin{cases} ma_1' = \alpha'_{mk}1s_N + \alpha'_{ms}2s_N + \alpha'_{mh}a_1'(H_3) \\ 1e' = \beta'_p 2p\pi_N + \beta'_h e'(H_3) \\ 1a_2'' = 2pz_N \end{cases} \qquad (4)$$

$$\text{with } a_1(H_3) = a_1'(H_3) = (1s_a + 1s_b + 1s_c)/[3(1 + 2S_h)]^{1/2}$$
$$e(H_3) = e'(H_3) = \begin{cases} (1s_a - 1s_b)/[2(1 - S_h)]^{1/2} \\ (1s_a + 1s_b - 2\cdot 1s_c)/[6(1 - S_h)]^{1/2} \end{cases} \qquad (5)$$

The AOs (atomic orbitals) $1s_N$, $2s_N$, $2pz_N$, $2p\pi_N$, are normalized N atom AOs, with $2p\pi_N$ representing a 2-fold degenerate pair, say $2px_N$ and $2py_N$. The z-axis lies in the symmetry axis of the molecule. The MO $1a_1$ or $1a_1'$ is nearly pure $1s_N$, while the other a_1 MOs are nearly free from $1s_N$.[8] Since the MO species e or e' is 2-fold degenerate, there are two $e(H_3)$ or $e'(H_3)$ GOs (group orbitals), which may conveniently be chosen as the two orthonormal forms given in (5), or in other ways. S_h in (5) is the overlap integral between any two adjacent H atoms.

It will be noted that in the passage from planar to pyramidal NH_3, the $1a_2''$ and the several a_1' MOs of planar NH_3 all become a_1 MOs (*cf.* Table II) and so become partially mixed (s-pz hybridization). In particular, $1a_2''$ goes over into $3a_1$, but undoubtedly $3a_1$ is still *mainly* composed of $2pz_n$, *i.e.*, α_{3s} in eq. 3 as applied to $3a_1$ is no doubt the largest coefficient. The fact that pyramidal NH_3 is more stable than planar NH_3 (but by only $^1/_4$ e.v.)[2b] may be attributed to an over-all gain in bond energy as a net result of s-pz mixing in the $2a_1$ and $3a_1$ MOs. (It seems probable that there is a strong increase in bonding power in going from $2a_1'$ to $2a_1$, but that the non-bonding $1a_2''$ becomes slightly antibonding in going to $3a_1$.)

LCAO MO theory thus makes it qualitatively understandable why the HNH angles in NH_3 are less than the 120° values of planar NH_3, but provides no ready explanation as to why they have just the observed value. Values of 90° or less would not be astonishing according to qualitative LCAO MO theory, according to which there is nothing critical about the angle 90°. In particular, 2s-2pz hybridization must still be present, presumably strong, and perhaps still increasing, in the a_1 MOs for 90° and smaller angles.

On the other hand, qualitative VB (valence-bond) theory, in its usual simple form assuming N–H bond directions to coincide with symmetry axes of AOs, would associate 90°, 109°28′, and 120° angles, respectively, with pure p valence, tetrahedral s-p hybridization, and trigonal s-p hybridization.[5]

Although qualitative LCAO theory does not explain why the pyramidalization of planar NH_3 stops at just 106°46′, it does reveal a factor which should markedly resist departure of NH_3 from planar form and so oppose the factor of s-pz hybridization in the a_1 MOs which favors such departure. This resisting factor arises from the fact that bonding in the strongly bonding 1e or 1e′ MOs of (1) or (2) should be at a maximum for planar NH_3. Two reasons for this can be seen from the form of these MOs (*cf.* 3, 4 and 5). Firstly, the bonding overlap between $2r\pi_N$ and $e(H_3)$ is somewhat larger for planar than for pyramidal NH_3; a computation gives 0.61 and 0.59 for the respective values of the overlap integral in the two cases. Secondly, there is an antibonding overlap, hence H–H repulsion energy, *within* the $e(H_3)$ GOs of (5), which increases strongly as the angle decreases. Assuming r_{NH} constant, the distance r_{HH} between any two H atoms is given by

$$r_{HH} = 2r_{NH}\sin\gamma/2 \qquad (6)$$

where γ is the bond angle. Knowing r_{HH}, the corresponding overlap integral S_h can be computed; the respective values are 0.29 and 0.33 for planar NH_3 and 106°46′ pyramidal NH_3.

Another approach to one of the factors which should affect the bond angle is to examine from the VB theory standpoint how the non-bonded repulsions between the H atoms change from planar to pyramidal NH_3. The non-bonded repulsion energy can be estimated as

$$\text{NBRE} = (3/2)AIS_h^2/(1 - S_h^2) \qquad (7)$$

using a semi-empirical formula which has been proposed in an earlier paper,[9] after introducing a factor 3 because there are three H–H non-bonded pairs. In (7), A is 0.65 and I is the ionization energy (13.60 e.v.) for an H atom. The following results are obtained (see Table III). An increase of 0.45 e.v. in H–H non-bonded repulsions on pyramidalization of NH_3 is indicated. However, it should be pointed out that Heath and Linnett,

(8) *Some* admixture of inner-shell and outer-shell AOs is necessary; see R. S. Mulliken, *J. Chem. Phys.*, **19**, 912 (1951).

(9) *Cf.* R. S. Mulliken, THIS JOURNAL, **72**, 4493 (1950), Section V and Table XI.

and Simanouti,[3] have cited evidence which seems to indicate that non-bonded repulsions between H atoms are unimportant in hydrides AH_n.

TABLE III

ESTIMATED NON-BONDED H–H REPULSION ENERGIES (NBRE)

NH_3				PH_3			
γ	r_{HH} (Å.)	S_h	NBRE (e.v.)	γ	r_{HH} (Å.)	S_h	NBRE (e.v.)
120°	1.76	0.29	1.21				
106° 46′	1.628	.33	1.66	93° 18′	2.06	0.20	0.57
90°	1.437	.41	2.65	90°	2.00	.22	.64

In comparing the results in Table III with our preceding LCAO considerations, it is necessary to realize that the H–H non-bonded repulsions of VB theory correspond in LCAO theory to the *net resultant* effect of (a) positive contributions, from H–H *bonding* within $a_1(H_3)$, to over-all bonding in the ma_1 set of MOs (*cf.* eq. 3 and 5); (b) negative contributions (see second preceding paragraph), from H–H *antibonding* within $e(H_3)$, to over-all bonding in the 1e MOs. The NBRE's of Table III correspond to the *excess* of (b) over (a).

Perhaps the best over-all approach is to use the LCAO viewpoint for the resonance interactions between N atom and H_3 group electrons, and the VB viewpoint for the interactions within the H_3 group.

Summarizing, pyramidalization should strongly stabilize the a_1 set of electrons in NH_3 by permitting s-pz hybridization, but destabilize the *e* set through decreasingly favorable overlap; further, it should destabilize by increasing the H–H non-bonded repulsions; the net result must be the observed slight (0.26 e.v.) stabilization at a pyramidal form with bond angle 106°46′.

Let us now turn to PH_3 as an example of the higher-row analogs of NH_3. The MO electron configuration is

planar PH_3:

$$(1a_1')^2(2a_1')^2(1e')^4(1a_2'')^2(3a_1')^2(2e')^4(2a_2'')^2 \qquad (8)$$

pyramidal PH_3:

$$(1a_1)^2(2a_1)^2(1e)^4(3a_1)^2(4a_1)^2(2e)^4(5a_1)^2 \qquad (9)$$
$$\text{B} \quad \text{B}$$

The four MOs occupied by the first ten electrons should be nearly the same as AOs of the inner shells of the phosphorus atom. The last eight electrons, in valence shell MOs, correspond to the last eight in configuration (1) or (2) for NH_3. But because 3d AOs are now available for hybridization, as they surely are not to an appreciable extent in NH_3, (3) and (4) are replaced, *for the valence-shell MOs*, by the following

$$\text{pyr. } PH_3\ (C_{3v}):\ \begin{cases} \text{ma} = \cdots + \alpha_{ms}3s_P + \alpha_{mz}3pz_P + \alpha_{md}3d\sigma_P + \alpha_{mh}a_1(H_3) \\ \text{2e} = \cdots + \beta_p 3p\pi_P + \beta_{d\delta}3d\delta_P + \beta_{d\pi}3d\pi_P + \beta_h e(H_3) \end{cases} \qquad (10)$$

$$\text{planar } PH_3\ (D_{3h}):\ \begin{cases} \text{ma}' = \cdots \alpha'_{ms}3s_P + \alpha'_{md}3d\sigma_P + \alpha'_{mh}a_1'(H_3) \\ \text{2e}' = \cdots + \beta'_p 3p\pi_P + \beta'_{d\delta}3d\delta_P + \beta'_h e'(H_3) \\ 2a_2'' = \cdots + 3pz_P \\ \text{1e}'' = 3d\pi_P \text{ (unoccupied)} \end{cases} \qquad (11)$$

The $\cdots$ in eq. 10 and 11 refer to slight admixtures[8] with inner-shell P atom AOs of proper symmetry. For $a_1(H_3)$ and $e(H_3)$, see eq. 5. The classification of the 3d AOs into $3d\sigma$, $3d\pi$, $3d\delta$ is based on their behavior with respect to rotations around the *z*-axis and reflections in planes through it. It will be noted that $3s\text{-}3d\sigma$ and $3p\pi\text{-}3d\delta$ hybridization can occur for *either* planar or pyramidal PH_3, and so may not appreciably favor the one form over the other. Further, however, in complete analogy to NH_3, 3s-3pz hybridization can occur for pyramidal but not for planar PH_3, and should cause stabilization of the pyramidal form in the same way as for NH_3.

Finally, a distinctive new feature appears in PH_3, namely, $3p\pi\text{-}3d\pi$ hybridization in the 2e MO, but only in the pyramidal form. Of considerable importance in this connection is the fact, which can readily be seen from the forms of the $3d\pi$ AOs, that their hybrids with $3p\pi$ can bend down and "follow" the H_3 group if the plane of the latter is moved down away from the P atom. Thus $3p\pi\text{-}3d\pi$ hybridization superposes on the resisting factor toward pyramidalization, which was noted above for the corresponding 1e valence-shell MOs of NH_3, a factor favoring pyramidalization. Further, even without $3p\pi\text{-}3d\pi$ hybridization, the resistance of the 2e MOs of PH_3 toward pyramidalization should be less than for the 1e MOs of NH_3, since the S_h values are smaller at all angles (*cf.* Table III).

Now turning to the VB approach, Table III indicates that the interhydrogen non-bonded repulsion energy, computed by eq. 7, is much smaller for PH_3 even at the observed bond angle near 90° than for NH_3 with its bond angle of 106°46′ or even than for planar NH_3. The indicated sharp decrease is a simple consequence of the large increase in size of the P atom as compared with the N atom, which is reflected in the observed bond distances (N–H, 1.014 Å.; P–H, 1.415 Å.),[2b] hence in the H–H distances and H–H overlaps.

Summarizing, pyramidalization of planar PH_3 should strongly stabilize the a_1 set of electrons by permitting s-pz hybridization (s-d hybridization is also present), and should also probably stabilize the e set of electrons by permitting $p\pi\text{-}d\pi$ hybridization; at the same time it should cause a little destabilization by increasing the H–H non-bonded repulsions; the net result must be the observed strong (1.3 e.v. as compared with planar PH_3)[2b] stabilization at a pyramidal form with bond angle 93°18′. As compared with NH_3, the pyramidal form should be favored by the incidence of $p\pi\text{-}d\pi$ hybridization, and by a decrease in H–H non-bonded repulsions due to the considerably larger size of the P than the N atom. Decreased electrostatic repulsions between the charges on the H atoms should be an additional minor factor. Similar considerations apply to AsH_3, SbH_3 and BiH_3. In AsH_3, the As–H bond distance is 1.52 Å., the bond angle is 91°30′, and the stabilization energy relative to planar AsH_3 is 1.5 e.v.[2b]

The explanation given here is of course a qualitative one, and does not specifically account for the fact that the bond angles seem to be approaching a limiting value of 90° in the higher-row fifth-column hydrides. However (see discussion above), LCAO theory suggests that this fact may be somewhat fortuitous.

Sixth-Column Hydrides

Paralleling the comparison between NH_3 and

PH_3, one can show that p-d hybridization affords a qualitatively reasonable explanation of the smaller bond angle in H_2S than in H_2O. For the latter, the electronic structure is

$$H_2O: (1a_1)^2(2a_1)^2(1b_2)^2(3a_1)^2(1b_1)^2 \quad (12)$$
$$\qquad\quad B \quad B$$

The principal bonding MOs are indicated by the letter B. The classification of the MOs is in accordance with the symmetry C_{2v}, and their forms, in LCAO approximation, are

$$H_2O: \left\{\begin{array}{l} ma_1 = \alpha_{mk}1s_O + \alpha_{ms}2s_O + \alpha_{mz}2pz_O + \alpha_{mh}a_1(H_2) \\ 1b_2 = \beta_y 2py_O + \beta_h b_2(H_2) \\ 1b_1 = 2px_O \end{array}\right\} \quad (13)$$

$$\text{with} \left\{\begin{array}{l} a_1(H_2) = (1s_a + 1s_b)/[2(1 + S_h)]^{1/2} \\ b_2(H_2) = (1s_a - 1s_b)/[2(1 - S_h)]^{1/2} \end{array}\right\} \quad (14)$$

The AOs $1s_O$, $2s_O$, $2px_O$, $2py_O$ and $2pz_O$ are normalized O atom AOs, while $a_1(H_2)$ and $b_2(H_2)$ are normalized GOs of the H_2 group. S_h is the overlap integral between the 1s AOs $1s_a$ and $1s_b$ of the two H atoms. The y- and z-axes are chosen in the plane of the molecule (see Fig. 1). H atoms a and b are centered in locations with positive and negative y, respectively. The MO $1a_1$ is nearly pure $1s_O$ (*i.e.* $\alpha_{1k} \approx 1$), while the other a_1 MOs are nearly free from $1s_O$ (*i.e*, $\alpha_{mk} \approx 0$).[8] Quantitative computed values for all the coefficients in (13) have been reported by Ellison and Shull.[10]

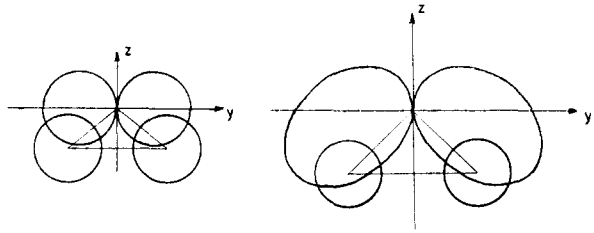

Fig. 1.—Skeletons of H_2O and H_2S drawn to scale. The b_2 AO $2py_O$ (for H_2O) and $3py\text{-}3d\pi_y$ hybrid S atom b_2 AO-(H_2S) and their overlap with the $b_2(H_2)$ GO (*cf.* eq. 14) are shown schematically.

For H_2S, the structure is

$$H_2S: (1a_1)^2(2a_1)^2(1b_2)^2(3a_1)^2(1b_1)^2(4a_1)^2(2b_2)^2(5a_1)^2(2b_1)^2 \quad (15)$$
$$\qquad\qquad\qquad\qquad\qquad\qquad\qquad\qquad B \quad B$$

The first ten electrons correspond approximately to the S atom inner shells, while the last eight, in valence shell MOs, correspond to the last eight electrons in configuration (12) for H_2O. But because 3d AOs are now available for hybridization, (13) is replaced, *for the valence-shell MOs*, by

$$H_2S: \left\{\begin{array}{l} ma_1 = \cdots + \alpha_{ms}3s_S + \alpha_{mz}3pz_S + \alpha_{md\delta}3d\sigma_S + \alpha_{md\delta}3d\delta a_1 + \alpha_{mh}a_1(H_2) \\ 2b_2 = \cdots + \beta_y 3py_S + \beta_d 3d\pi_y + \beta_h b_2(H_2) \\ 2b_1 = \cdots + \gamma_x 3px_S + \gamma_d 3d\pi_x \end{array}\right\} \quad (16)$$

The classification of the 3d AOs into $3d\sigma$, $3d\pi$ and $3d\delta$ is based on their behavior with respect to rotations around the z-axis and reflections in planes through it.

Comparison of the LCAO MOs of H_2O and H_2S with those of NH_3 and PH_3 discloses a strong parallelism which indicates that the same factors may reasonably account for the smaller bond angles of the second-row-atom hydrides in both pairs, with the a_1 and b_2 sets of MOs in H_2O and H_2S performing much like the a_1 and e sets in NH_3 and PH_3. The analog of planar structures for NH_3 and PH_3 would be linear symmetrical structures (bond angle 180°) for H_2O and H_2S, but of course the latter molecules are much farther from being linear structures than are the former from being planar structures. Nevertheless, it is worth noting that in the a_1 MOs of H_2O and H_2S, s-pz hybridization would vanish in the linear case but become strong with decreasing bond angle; while in the b_2 MOs bonding between py_O or py_S and $b_2(H_2)$ would be a maximum in the linear case. In eq. 14, H–H bonding in the a_1 MOs and H–H antibonding in the b_2 MOs increase with decreasing angle. For these reasons, the a_1 MOs should favor a small but the b_2 MO a large bond angle in H_2O.

In H_2S, d hybridization enters as a new factor which in the $2b_2$ MO strongly favors a decreased bond angle, since $3py\text{-}3d\pi_y$ hybridization (like $3p\pi\text{-}3d\pi$ hybridization in the 2e MOs of PH_3) increases with decreasing angle, and enables the resulting hybrid b_2 sulfur atom AO to "follow" the H atoms as the angle sharpens (*cf.* Fig. 1). There is also d hybridization in the a_1 MOs ($3d\sigma$ for all angles, $3d\delta$ for angles $<180°$). Burns and Gordy[5] also have previously postulated that d hybridization is important in H_2S.

Another factor which should favor a smaller bond angle in H_2S is decreased H–H non-bonded repulsion (*cf.* Table IV), in spite of the smaller bond angle. This can be estimated using

$$\left.\begin{array}{l} r_{HH} = 2r_{OH}\sin\gamma/2 \text{ or } 2r_{SH}\sin\gamma/2 \\ \text{NBRE} = {}^1/_2 AIS_h^2/(1 - S_h^2) \end{array}\right\} \quad (17)$$

similar to eq. 6 and 7; but see remarks following Table III.

TABLE IV

ESTIMATED NON-BONDED H–H REPULSIONS (NBRE)

	H_2O				H_2S		
	r_{HH}		NBRE		r_{HH}		NBRE
γ	(Å.)	S_h	(e.v.)	γ	(Å.)	S_h	(e.v.)
105° 3′	1.518	0.37	0.72	92° 16′	1.925	0.24	0.27
90°	1.356	.44	1.07	90°	1.890	.25	.29

Summarizing, the incidence of p-d hybridization in the b_2 MOs, and decreased H–H non-bonded repulsions, should favor a smaller bond angle for H_2S than for H_2O, and may reasonably be supposed to be the main causes for the observed smaller angle. The same factors should favor even slightly smaller angles for H_2Se and H_2Te.

Fifth- and Sixth-Column Halides

The bond angles in the derivatives of the fifth- and sixth-column halides are less easy to understand than those of the hydrides, since the additional valence-shell electrons in the substituent atoms bring new possibilities of interaction. However, the fifth-column-atom halides will be considered briefly here. For NF_3, if it were planar, the MO structure would be

(10) F. O. Ellison and H. Shull, *J. Chem. Phys.*, **21**, 1420 (1953). Their calculations show that Walsh's MO energy diagram for AH_2 molecules (see ref. 4) is very far from quantitatively correct.

$$(1a_1'[1s_F])^2(1e'[1s_F])^4(2a_1'[1s_N])^2(3a\ [2s_F])^2(2e'[2s_F])^4\ (18)$$
$$(4a_1')^2(3e')^4(1a'')^2(1e''[2pz_F])^4(1a_2'[2py_F])^2(4e'[2py_F])^4(2a\ )^2$$
$$\text{B}\quad\text{B}\quad\text{B}\qquad\qquad\qquad\qquad\text{A}$$

Most of the MOs are non-bonding or nearly so, and correspond approximately to F_3 GOs formed from sets of the F atom AOs indicated in brackets, or in the case of $2a_1'$ to an N atom 1s AO; the reference axes for the various atoms are shown in Fig. 2. The MOs $4a_1'$, $3e'$, and $1a_2''$, marked B, are bonding, while $2a_2''$, marked A, is antibonding.

With the omission of the last two electrons and with obvious changes in the atomic labels, (18) describes the structure of the planar molecules BF_3, $CO_3^=$, NO_3^-, which then have four pairs of bonding electrons, or, in VB theory language, four bonds (one double bond and two single bonds, with resonance) from the central atom. Inclusion of the $2a_2''$ electrons, as in planar NF_3, should (more than) cancel the bonding effect of the $1a_2''$ electrons, leaving essentially three bonds. Empirically, these evidently are somewhat strengthened on going over to pyramidal NF_3.

The forms of the bonding and antibonding MOs in (18) are in LCAO approximation

$$\left.\begin{aligned} 4a_1' &= \cdots + \alpha_s\, 2s_N + \alpha_f a_1'(xF_3) \\ 3e' &= \cdots + \beta_p\, 2p\pi_N + \beta_f e'(xF_3) \\ 1a_2'' &= \gamma_z\, 2pz_N + \gamma_f a_2''(zF_3) \\ 2a_2'' &= \delta_f\, a_2''(zF_3) - \delta_z 2pz_N \end{aligned}\right\} \qquad (19)$$

where $a_1'(xF_3)$ and $a_2''(zF_3)$ are similar to $a_1'(H_3)$ in eq. 5 but are constructed from sets of $2px_F$ and $2pz_F$ AOs, respectively, instead of from $1s_H$ sets, $e'(xF_3)$ is like $e'(H_3)$ in eq. 5 but constructed from $2px_F$ instead of $1s_H$ sets.[11]

In actual pyramidal, NF_3, there is mixing between some of the MOs of (18), —a_1' and a_2'' both become a_1, e' and e'' become e, and a_2' becomes a_2 (*cf.* Table II),—and (18) becomes

$$(1a_1)^2(1e)^4(2a_1)^2(3a_1)^2(2e)^4(4a_1)^2(3e)^4(5a_1)^2(4e)^4(1a_2)^2$$
$$\text{B}\quad\text{B}$$
$$(5e)^4(6a_1)^2 \qquad (20)$$

Pyramidalization may be attributed partly or largely to essentially the same factors as in NH_3 ($2s_N$–$2pz_N$ hybridization which becomes possible when a_2'' mixes with a_1', both becoming a_1). However, the mixings are more complicated than in NH_3, because of the extra electrons from the fluorine valence shells. In particular, the presence of $1e''$ in (18), which can mix with $3e'$ on pyramidalization, may well reduce the resistance to pyramidalization which characterizes $1e'$ of NH_3.

Non-bonded repulsions between F atoms in NF_3 would be expected theoretically to be smaller than between H atoms in NH_3, since, although there are more valence-shell electrons, the F atoms in NF_3 are both smaller and farther apart than the H atoms in NH_3. This difference may perhaps be the main reason for the somewhat smaller valence angles in NF_3 than in NH_3.

(11) The $\cdots$ in $4a_1'$ represents a linear combination of $a_1'(1sF_3)$ and especially $a_1'(2sF_3)$ in small amounts, and $\cdots$ in $3e'$ represents a linear combination of $e'(1sF_3)$, $e'(yF_3)$, and especially $e'(2sF_3)$, in small amounts.

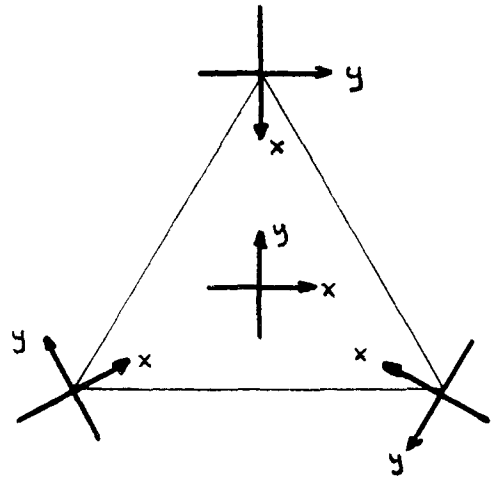

Fig. 2.—Local reference axes for atoms in planar AB_3. All z-axes point upward.

For PF_3, MO electron configurations essentially like (18) and (20) except for augmentation by electrons corresponding to $2s_P^2 2p_P^6$ can easily be written. Hybridization with $3d_P$ AOs now also enters, but in contrast to PH_3, d hybridization can occur in *all* the MOs (except $1a_2'$) for both planar and pyramidal PF_3; $d\sigma$ can mix into a_1', $d\delta$ into e', and $d\pi$ into e'' for planar PF_3; or $d\sigma$ into a_1, $d\delta$ and $d\pi$ into e, for pyramidal PF_3. Thus d hybridization may be a less important factor favoring pyramidalization than in PH_3. However, as in the latter, it should at any rate give some added strength to the bonds, equivalent in part to partial double bonding in VB theory language.

The fact that the bond angle does not decrease from NF_3 to PF_3 and AsF_3 (*cf.* Table I) may perhaps be attributed to the existence of appreciable and increasing electrostatic repulsions among the F atoms; the P–F and As–F electronegativity differences are large, making the charges on the F atoms here much larger than on the H atoms in PH_3 and AsH_3, and considerably larger than on the F atoms in NF_3.

Similar considerations apply to the halides of sixth-row atoms. The exceptionally large bond angle for Cl_2O (larger than for F_2O, *cf.* Table I) seems most reasonably attributable to the relatively large size of the Cl atoms, hence to unusually large non-bonded repulsions. It is also reasonable to believe that these repulsions are not so important in most of the other halides.

Although the foregoing discussion of the halides is sketchy, it touches on most of the factors which seem likely to be important in controlling the bond angles. Because of the complexity of these factors, a more detailed discussion would scarcely be justified.

CHICAGO, ILLINOIS